11th International Conference on Power Electronics-ECCE Asia
May 22 - 25, 2023 / ICC Jeju, Jeju, Korea

A Single-Stage Soft-Switched LVDC to Three-Phase MVAC Converter for MV Grid Integration of Utility-Scale Solar PV

Surjakanta Mazumder
Department of Electrical Engineering
Indian Institute of Science, Bangalore
Bangalore, India
surjakantam@iisc.ac.in

Anirban Pal
GE Aerospace
Bangalore, India
anirban.pal@ge.com

Kaushik Basu
Department of Electrical Engineering
Indian Institute of Science, Bangalore
Bangalore, India
kbasu@iisc.ac.in

***Abstract*— This paper presents a single-stage high-frequency link multi-level three-phase DC-AC converter for medium voltage grid integration of utility-scale solar park. On the DC side, three half-bridge legs are used. The converter employs three high-frequency transformers with multi-winding secondaries to provide galvanic isolation between the DC and AC sides. The output of each secondary winding is fed to an active rectifier followed by a full-bridge-based unfolder circuit to generate the line frequency AC. The rectifier-unfolder stages are then connected in cascade to build the medium voltage AC before connecting to the MV utility grid through line filters. The modulation strategy ensures zero-voltage switching of the DC side half-bridge legs throughout the line cycle. For DC-AC power flow, the secondary active rectifiers are soft-switched, and the unfolder circuits are line frequency switched, thus incurring negligible switching loss. The converter avoids using a bulky interstage DC-link filter capacitor. The operation of the converter is verified in MATLAB simulation, and critical simulation results are given in the paper.**

***Index Terms*—Single stage high frequency link, DC-AC Converter, Medium voltage grid integration, Utility scale PV.**

I. Introduction

Multi-level, high-frequency-link (HFL) DC-AC power converters are becoming popular for direct medium voltage grid integration of renewable sources e.g utility scale solar and wind parks etc [1], [2]. These converters employ high frequency transformers (HFT) to match the voltage levels and to provide galvanic isolation between the DC and AC sides. Additionally, the galvanic isolation ensures reduced leakage and circulating currents between the PV modules. Traditionally a three-phase inverter along with a line frequency step-up transformer is used for such applications [3], [4]. In comparison, the high-frequency-link based DC-AC power converters provide high power density, light weight converter solution.

Several multi-level HFL topologies are widely explored in literature. Based on the converter structure, these are broadly classified in two groups- multi-stage and single stage topology. In multi-stage multi-level topology, a cell is realized with an isolated DC-DC stage followed by a DC-AC stage connected through inter-stage DC link capacitor. Several such cells are connected in cascade to build the medium voltage AC [2]- [8]. The isolated DC-DC stage can be implemented with a DAB, PSFB or LLC converter.

The DC-DC and DC-AC stage can have either two or three level configurations. In [6]- [8], multi-winding high frequency transformers are used to reduce number of cells in the DC-DC converter. Major drawbacks of multi-stage topology are higher filtering requirement, capacitor life related long term reliability issue etc. In a single stage topology, the interstage DC link capacitors are avoided [9]- [11]. Here in the AC side of a cell, a cycloconverter can be used to directly converter HF AC to line frequency AC. Sometimes a rectifier followed by an inverter is used without any interstage DC capacitor and hence the interstage DC link is pulsating.

For PV application, due to unidirectional nature of power flow, PSFB is a popular choice [11]–[14] for the isolated DC-DC stage. Here the input bridge is soft-switched where ZVS is achieved with the help of device capacitance and transformer leakage inductance. But the ZVS is load dependent. During light load, the energy stored in the transformer leakage inductance is not sufficient to charge and discharge the device capacitor resulting into hard switching of the converter. To achieve ZVS, additional passive [15]–[17] and active [18]–[20] snubber circuits are employed. In the literature, several PSFB based single stage DC-AC converter solutions are proposed [11], [12]. Here the converter is hard switched near the zero crossing of line current even for the rated load. Auxiliary inductor based passive snubber circuits are employed to increase the ZVS range over the line cycle in [21], [22].

One of the significant disadvantages of existing topologies is they employ many cells hence, power devices, albeit lower voltage and power rating [10], [11]. In this paper a new isolated, three phase, single stage multi-level topology is proposed. Some key features are as follows. a) The converter employs only three half bridge legs in the LV DC side. b) Sinusoidal pulse width modulation (PWM) is implemented in the DC side bridge. These half-bridge legs are phase-shift modulated. c) The modulation strategy ensures zero voltage switching of all six switches of the DC side half-

bridge legs over complete line cycle without any external snubber. d) Three multi-winding high frequency transformers are used for the three phases. e) In the AC side, active rectifier followed by unfolder (line frequency switched inverter) stages are employed. Thus, incurring negligible switching loss. f) The converter does not employ filter capacitors, thus improving the converter reliability.

The paper is organized as follows. Section II describes the proposed power architecture. The modulation strategy is detailed adequately in Section III. The efficacy of the power converter is verified through simulation and the corresponding results are presented in Section IV. Finally, the article is concluded in Section V.

II. Proposed Topology

The complete power architecture of the proposed high-frequency DC-MVAC system is shown in Fig.1. On the DC side, there are three half-bridge legs. Three multi-winding high-frequency transformers are used, each with a single primary and p number of secondaries. The primary windings of the transformers are connected in delta, and the secondaries are directly connected to the active rectifiers, followed by line frequency inverter-unfolder stages. The output of un-folder stages in a phase are connected in cascade through LC filters before connecting them to the medium voltage grid. The specifications of the power architecture are tabulated in Table. I.

TABLE I
SPECIFICATIONS OF THE PROPOSED MVAC ARCHITECTURE

Output Power, P	100 kW
Input Voltage, V_{DC}	800 V
Output Voltage, (v_{L-L})	3.3 kV
Fundamental Frequency, f_o	50 Hz
Switching Frequency, f_s	40 kHz

III. Modulation Strategy

The purpose of the modulation strategy is to generate high-quality sinusoidal voltage v_{aN}, which can track the given reference voltage $v_{ref,a} = V_{pk}\sin(\omega t)$, where ω is the angular frequency of grid voltage. ωt is defined as the grid angle, denoted as θ. The reference voltages of the other two phases are $\pm 120^o$ apart from each other. The modulation signal is the rectified sine wave and can be expressed in (1), where $m = \left(\frac{V_{pk}}{npV_{DC}}\right)$.

$$m_a = m|\sin\theta| \tag{1}$$

Here, n, p, and V_{DC} are defined for the secondary to primary turns ratio, the number of secondary cells connected in series in each phase, and DC bus voltage, respectively. Similarly, for the other two phases, the modulation signals can be expressed as $m_b = m|\sin(\theta - 120^o)|$ and $m_c = m|\sin(\theta + 120^o)|$, respectively.

The half-bridge legs on the DC side are phase-shift modulated, and the devices of each leg are complementary switched with square wave gating pulses of 50% duty ratio and period T_s. The transformer flux is balanced over $T_s = \frac{1}{f_s}$, where f_s is much higher than 50 Hz.

TABLE II
REFERENCE LEG SELECTION

θ	$108^o - 240^o$	$240^o - 300^o$	$300^o - 360^o$
	$0^o - 60^o$	$60^o - 120^o$	$120^o - 180^o$
Reference Leg	U	W	V

From Fig. 2, it is observed that the gating signal of S_V is shifted to S_U by $0.5m_aT_s$, resulting in applied a quasi-square wave voltage with levels $\pm V_{dc}$, 0 and pulse width $0.5m_aT_s$ across the transformer primary winding, UV. In the secondary, the first bridge rectifies the high-frequency AC input into the pulsating DC output, which is given as $v_{a1} = n|v_{UV}|$. Then, the unfolder does the line frequency inversion of v_{a1}. The output of the un-folder is represented in (2), where sgn(x) is the sign of signal x.

$$v_{a2} = v_{a1} \cdot sgn(v_{ref,a}) \tag{2}$$

The L-C filter is introduced to eliminate the high-frequency switching ripple. Due to series connection, the output of all p modules of phase a is added to generate v_{aN}, which can be expressed in (3) where, $\overline{v}$ is the switching cycle average of waveform v.

$$v_{aN} = p\overline{v}_{a2} = nmpV_{DC}\sin\theta = v_{ref,a} \tag{3}$$

Similarly, the gating signal of S_W is phase-shifted to S_U by $0.5m_cT_s$ (shown in Fig.2), which ultimately applies a quasi-square wave voltage v_{UW} across the transformer primary terminal UW. Applying KVL across the delta-connected primary of the high-frequency transformer, the relation between v_{UW}, v_{WV}, v_{VU} can be expressed in (4).

$$v_{VW} = v_{UW} - v_{UV} \tag{4}$$

For the considered switching period $m_b = m_a - m_c$ and hence a quasi-square voltage v_{VW} of pulse width $0.5m_bT_s$ is automatically applied across VW terminal of the transformer (see Fig. 2). If m_{max}, m_{mid}, and m_{min} are the maximum, medium and minimum of m_a, m_b, m_c, they are related as follows in (5).

$$m_{max} = m_{mid} + m_{min} \tag{5}$$

For the considered switching instant (see Fig. 2, the $m_{max} = m_a$, $m_{mid} = m_b$, $m_{min} = m_c$, and the reference leg is U ($S_U - S'_U$). As m_a, m_b, m_c vary sinuously over a line cycle, the reference needs to be changed at every 60^o to follow the described modulation strategy, shown in Table. II. For DC to AC side power flow, the primary half-bridges, active rectifiers, and unfolders form similar switching-cycle equivalent circuits like a PSFB converter, where the device capacitances and transformer leakage inductances are sufficient to get the soft-switching.

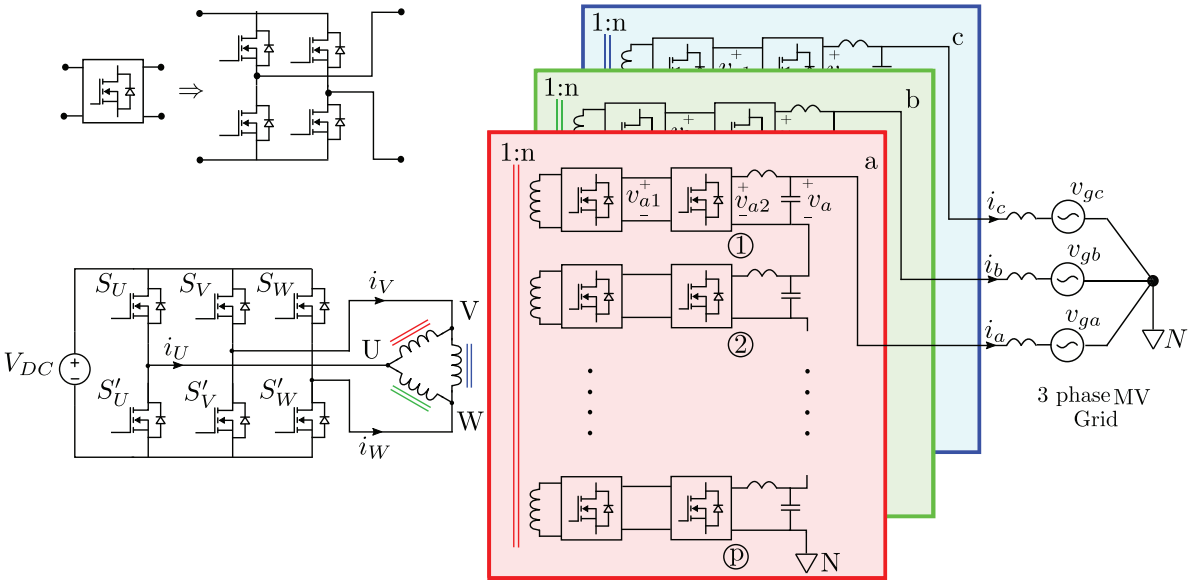

Fig. 1. Circuit diagram of the proposed high frequency link DC-MVAC converter

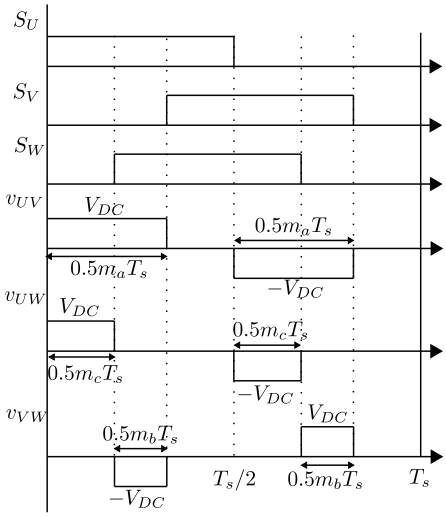

Fig. 2. Switching Signal Generation

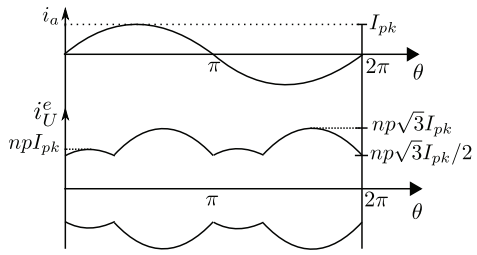

Fig. 3. Envelope of DC Side Leg Current

Fig. 3 shows the pole current envelope of the DC side half-bridge leg. The magnitude of the envelope is always greater than $\frac{\sqrt{3}npI_{pk}}{2}$, ensuring the ZVS of DC side half-bridge devices throughout the entire line cycle [12]. Here, I_{pk} is the peak of the line current.

IV. Results and Discussion

The operation of the proposed converter is verified using MATLAB simulation. The converter is simulated with 800 V DC input and transfers 100 kW power to a 3.3 kV AC grid. The switching frequency is 40 kHz. The transformer turns ratio is taken as 1:1.45. In the secondary, in each phase, three modules are connected in series to get the desired voltage level. The modulation index is kept at 0.9.

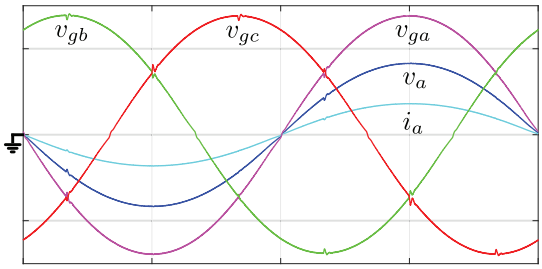

Fig. 4. v_{ga}, v_{gb}, v_{gc} (2 kV/div); i_a (65 A/div); v_a (1 kV/div); x-axis: 10 ms/div.

The three-phase output voltages (v_{ga}, v_{gb}, v_{gc}), output current (i_a), and output voltage (v_a) of a single module of phase a are presented in Fig. 4. The peak of v_a is at 892.93 V, and after connecting three of such modules in series (3 $\times$ 892.93=2678.78 V), it ensures 3.32 kV ($\frac{2678.78}{\sqrt{2}} \times \sqrt{3}$) L-L AC bus voltage.

Fig. 5 presents the primary voltages of the three phases (v_{UV}, v_{VW}, v_{WU}) along with the pole current of leg-U (i_U). This verifies the modulation strategy described in section II over two switching cycles. As seen from Fig. 5, $v_{UV} + v_{VW} + v_{WU} = 0$.

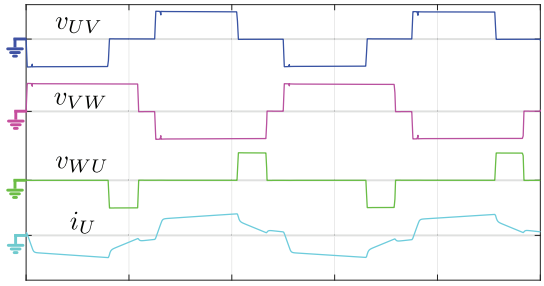

Fig. 5. v_{UV}, v_{VW}, v_{WU} (1 kV/div); i_U (200 A/div); x-axis: 10 μ s/div.

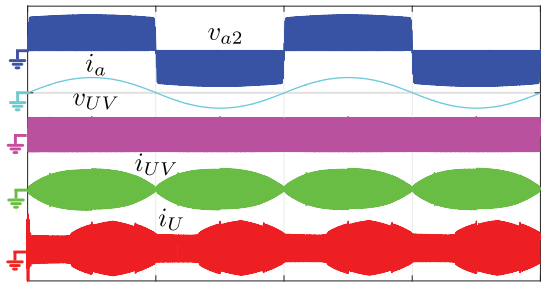

Fig. 6. v_{a2} (1.5 kV/div); i_a (65 A/div); v_{UV} (1 kV/div), i_{UV} (100 A/div); i_U (200 A/div); x-axis: 10 ms/div.

In Fig. 6, the output voltage of the unfolder stage (v_{a2}), line current (i_a), transformer primary voltage (v_{UV}), primary current (i_{UV}) and pole current of leg-U (i_U) is shown. It can be observed that i_U never touches the zero axis like i_{UV}, which ensures soft-switching throughout the line cycle of DC side half-bridges.

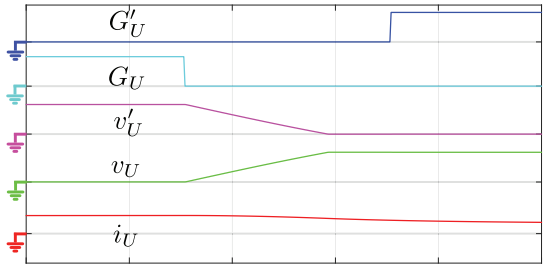

Fig. 7. G_U, G'_U (10 V/div); v_U, v'_U (1 kV/div); i_U (200 A/div); x-axis: 100 ns/div.

Soft-switching operation of the converter is observed in Fig. 7. The voltage of the bottom device of leg-U (v'_U) is fallen to zero before applying the gate pulse (G'_U), ensuring the ZVS turn-on of S'_U.

In Fig.8, different current waveforms consisting of load current (i_a) followed by primary currents (i_{UV}, i_{WU}) and then pole current of leg-U (i_U) are presented. In Fig.9, the voltage waveforms of different stages are presented, starting from primary side voltage (v_{UV}) followed by rectified voltage in the secondary (v_{a1}), then the voltage after un-folder (v_{a2}), followed by the the output voltage of single module (v_a). Which validates the complete power flow of this power architecture.

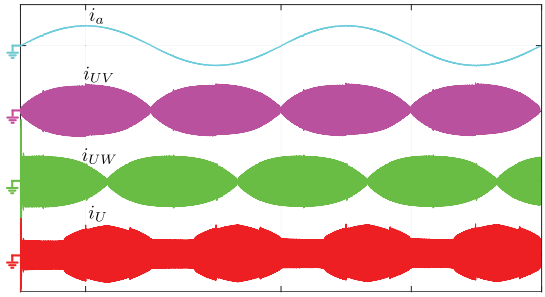

Fig. 8. i_a (65 A/div); i_{UV} (100 A/div); i_{WU} (100 A/div); i_U (200 A/div); x-axis: 10 ms/div.

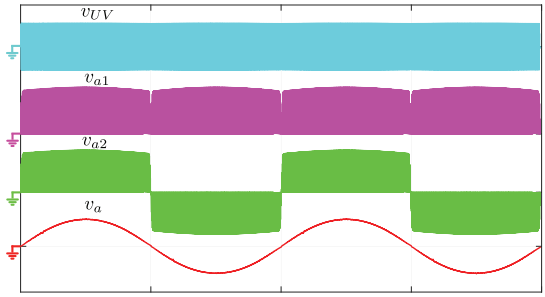

Fig. 9. v_{UV} (1 kV/div); v_{a1}, v_{a2}, v_a (1.5 kV/div); x-axis: 10 ms/div.

V. Conclusion

In this paper, a single-stage high-frequency link multi-level three-phase DC-AC converter is proposed. The modulation strategy presented in the paper ensures ZVS switching of the DC side active devices throughout the line cycle. AC side active devices are either zero voltage switched or line frequency switched, resulting in negligible switching losses. The cascaded secondary structure enables the converter to generate MV AC output allowing direct medium voltage grid integration. The converter employs high-frequency galvanic isolation, thus improving power density. Operation of the converter is discussed in detailed. Key simulation results are provided to validate the converter operation.

References

[1] D. Rothmund, T. Guillod, D. Bortis, and J. W. Kolar, "99.110 kv sic-based mediumvoltage zvs bidirectional single-phase pfc ac/dc stage," IEEE Journal of Emerging and Selected Topics in Power Electronics, vol. 7, no. 2, pp. 779-797, 2019.

[2] X. She, X. Yu, F. Wang, and A. Q. Huang, "Design and demonstration of a 3.6-kv 120- v/10-kva solid-state transformer for smart grid application," IEEE Transactions on Power Electronics, vol. 29, no. 8, pp. 3982-3996, 2014.

[3] S. Kouro, J. I. Leon, D. Vinnikov, and L. G. Franquelo, "Grid-connected photovoltaic systems: An overview of recent research and emerging pv converter technology," IEEE Industrial Electronics Magazine, vol. 9, no. 1, pp. 47-61, 2015.

[4] C. A. Rojas, S. Kouro, M. A. Perez, and J. Echeverria, "Dc-dc mmc for hvdc grid interface of utility-scale photovoltaic conversion systems," IEEE Transactions on Industrial Electronics, vol. 65, no. 1, pp. 352-362, 2018.

[5] L. F. Costa, G. Buticchi, and M. Liserre, "Quad-active-bridge dc-dc converter as crosslink for medium-voltage modular inverters," IEEE Transactions on Industry Applications, vol. 53, no. 2, pp. 1243-1253, 2017.

[6] L. F. Costa, G. Buticchi and M. Liserre, "Optimum design of a multiple-active-bridge dc-dc converter for smart transformer," IEEE Transactions on Power Electronics, vol. 33, no. 12, pp. 10 112-10 121, 2018.
[7] L. F. Costa, F. Hoffmann, G. Buticchi, and M. Liserre, "Comparative analysis of multiple active bridge converters configurations in modular smart transformer," IEEE Transactions on Industrial Electronics, vol. 66, no. 1, pp. 191-202, 2019.
[8] P. K. Achanta, B. B. Johnson, G. Seo, and D. Maksimovic, "A multilevel dc to threephase ac architecture for photovoltaic power plants," IEEE Transactions on Energy Conversion, vol. 34, no. 1, pp. 181-190, 2019.
[9] K. V. Iyer, R. Baranwal, and N. Mohan, "A high-frequency ac-link single-stage asymmetrical multilevel converter for grid integration of renewable energy systems," IEEE Transactions on Power Electronics, vol. 32, no. 7, pp. 5087-5108, 2017.
[10] M. Mahapatra, A. Pal, and K. Basu, "Soft switched multilevel unidirectional high frequency link dc/ac converter for medium voltage grid integration," in 2018 IEEE International Conference on Industrial Electronics for Sustainable Energy Systems (IESES), 2018, pp. 162-167.
[11] A. Pal and K. Basu, "A unidirectional single-stage three-phase soft-switched isolated dc-ac converter," IEEE Transactions on Power Electronics, vol. 34, no. 2, pp. 1142-1158, 2019.
[12] A. Pal and K. Basu, "A Soft-Switched High-Frequency Link Single-Stage Three-Phase Inverter for Grid Integration of Utility Scale Renewables," in IEEE Transactions on Power Electronics, vol. 34, no. 9, pp. 8513-8527, Sept. 2019.
[13] U. R. Prasanna and A. K. Rathore, "A novel single-reference six-pulsemodulation (SRSPM) technique-based interleaved high-frequency threephase inverter for fuel cell vehicles," IEEE Trans. Power Electron., vol. 28, no. 12, pp. 5547–5556, Dec. 2013.
[14] S. K. Mazumder, "Hybrid modulation scheme for a high-frequency aclink inverter," IEEE Trans. Power Electron., vol. 31, no. 1, pp. 861–870, Jan. 2016.
[15] O. D. Patterson and D. M. Divan, "Pseudo-resonant full bridge dc/dc converter," IEEE Trans. Power Electron., vol. 6, no. 4, pp. 671–678, Oct. 1991.
[16] P. K. Jain, W. Kang, H. Soin, and Y. Xi, "Analysis and design considerations of a load and line independent zero voltage switching full bridge dc/dc converter topology," IEEE Trans. Power Electron., vol. 17, no. 5, pp. 649–657, Sep. 2002.
[17] A. Safaee, P. Jain, and A. Bakhshai, "A ZVS pulsewidth modulation fullbridge converter with a low-rms-current resonant auxiliary circuit," IEEE Trans. Power Electron., vol. 31, no. 6, pp. 4031–4047, Jun. 2016.
[18] J. G. Cho, J. A. Sabate, and F. C. Lee, "Novel full bridge zero-voltagetransition PWM dc/dc converter for high power applications," in Proc. 9th Annu. IEEE Appl. Power Electron. Conf. Expo., 1994, pp. 143–149.
[19] A. F. Bakan, N. Altinta¸ s, and I. Aksoy, "An improved PSFB PWM dc–dc converter for high-power and frequency applications," IEEE Trans. Power Electron., vol. 28, no. 1, pp. 64–74, Jan. 2013.
[20] I.-O. Lee and G.-W. Moon, "Soft-switching dc/dc converter with a full ZVS range and reduced output filter for high-voltage applications," IEEE Trans. Power Electron., vol. 28, no. 1, pp. 112–122, Jan. 2013.
[21] S. Guo, J. Su, X. Chen, and X. Yu, "Soft-switching single-stage three-level power amplifier for high-voltage audio distribution systems," Electron. Lett., vol. 52, no. 21, pp. 1797–1799, 2016.
[22] S. Guo, J. Su, J. Lai, and X. Yu, "Analysis and design of a wide-range soft switching high-efficiency high-frequency-link inverter with dualphase-shift modulation," IEEE Trans. Power Electron., vol. 33, no. 9, pp. 7805–7820, Sep. 2018.
[23] R. Huang and S. K. Mazumder, "A soft switching scheme for multiphase dc/pulsating dc converter for three-phase high-frequency-link pulsewidth modulation (PWM) inverter," IEEE Trans. Power Electron., vol. 25, no. 7, pp. 1761–1774, Jul. 2010.